Applied Surface Science 447 (2018) 548–553

Contents lists available at ScienceDirect

Applied Surface Science

journal homepage: www.elsevier.com/locate/apsusc

Perspective Article

The Gaussian-Lorentzian Sum, Product, and Convolution (Voigt) functions in the context of peak fitting X-ray photoelectron spectroscopy (XPS) narrow scans

Varun Jain [a], Mark C. Biesinger [b], Matthew R. Linford [a,*]

[a] Department of Chemistry and Biochemistry, Brigham Young University, Provo, UT 84602, USA
[b] Surface Science Western, The University of Western Ontario, London, Ontario N6G 0J3, Canada

ARTICLE INFO

Article history:
Received 10 January 2018
Revised 22 March 2018
Accepted 23 March 2018
Available online 29 March 2018

Keywords:
XPS
GLS
GLP
Voigt function
Gaussian function
Lorentzian function

ABSTRACT

X-ray photoelectron spectroscopy (XPS) is arguably the most important vacuum technique for surface chemical analysis, and peak fitting is an indispensable part of XPS data analysis. Functions that have been widely explored and used in XPS peak fitting include the Gaussian, Lorentzian, Gaussian-Lorentzian sum (GLS), Gaussian-Lorentzian product (GLP), and Voigt functions, where the Voigt function is a convolution of a Gaussian and a Lorentzian function. In this article we discuss these functions from a graphical perspective. Arguments based on convolution and the Central Limit Theorem are made to justify the use of functions that are intermediate between pure Gaussians and pure Lorentzians in XPS peak fitting. Mathematical forms for the GLS and GLP functions are presented with a mixing parameter *m*. Plots are shown for GLS and GLP functions with mixing parameters ranging from 0 to 1. There are fundamental differences between the GLS and GLP functions. The GLS function better follows the 'wings' of the Lorentzian, while these 'wings' are suppressed in the GLP. That is, these two functions are not interchangeable. The GLS and GLP functions are compared to the Voigt function, where the GLS is shown to be a decent approximation of it. Practically, both the GLS and the GLP functions can be useful for XPS peak fitting. Examples of the uses of these functions are provided herein.

1. Introduction

X-ray photoelectron spectroscopy (XPS) is arguably the most popular and important high vacuum surface analytical tool [1]. It is unique in being highly surface sensitive, quantitative, and available in many laboratories and facilities, providing the elemental compositions of all the elements except helium and hydrogen, and yielding chemical/oxidation state information about the elements it detects [2]. Important decisions in the laboratory and in industry are made based on XPS results [3], where much of the key information derived from XPS is based on peak fitting narrow (high resolution) scans. Indeed, as explained by Sherwood, peak fitting is an indispensable part of XPS data analysis because the chemical shifts that provide the rich chemical information available through the technique and the widths of the fit components have comparable values [4]. For many years XPS practitioners have employed a variety of functions/peak shapes in their fitting. These have included pure Lorentzians, which model the fundamental/theoretical line shape, pure Gaussians, which often model amorphous materials well, e.g., polymers and glasses, Gaussian-Lorentzian sum and product functions, which consist of either the sum [5] or product [4] of these two functions, Voigt functions, which are the convolutions of Gaussian and Lorentzian functions, and other more complex functions, including the Doniach-Sunjic line shape [6]. Asymmetry must often be added to fit components/peaks to model conducting materials [7].

In this paper we discuss five functions that have been widely explored and used in XPS peak fitting: the Gaussian function, the Lorentzian function, the Gaussian-Lorentzian sum function (GLS), the Gaussian-Lorentzian product (GLP) function, and the Voigt function, which is a convolution of Gaussian and Lorentzian functions. A primary goal of this work is to compare the GLS and GLP functions. Indeed, different software packages for XPS peak fitting have different mathematical functions available in them. Thus, it is important to understand these synthetic line shapes, i.e., to know where they are best used and how to apply them. Arguments based on convolution and the Central Limit Theorem are made to justify the use of functions that are intermediate between pure Gaussians and pure Lorentzians in XPS peak fitting. This is

* Corresponding author.
E-mail address: mrlinford@chem.byu.edu (M.R. Linford).

https://doi.org/10.1016/j.apsusc.2018.03.190
0169-4332/

illustrated graphically by showing the results of the repeated convolution of a rectangle (slit) function with itself. Mathematical forms for the GLS and GLP functions are presented, where they each contain a mixing parameter, m, that ranges from 0 to 1. Plots are shown for the GLS and GLP functions with different values of the mixing parameter. The GLS function better follows the 'wings' of the Lorentzian, while, because of the more compact nature of the Gaussian function, these 'wings' are suppressed in the GLP. The GLS and GLP are compared to the Voigt function, where the GLS is shown to be the better approximation of it. Thus, there are fundamental differences between the GLS and GLP functions, i.e., they are not interchangeable. As shown below, both have their place in XPS peak fitting.

Finally, while peak fitting plays a central role in the work up and interpretation of XPS data, the use of other statistical tools and mathematical analyses of XPS peaks and data are also important [8,9]. These include chi squared, calculating and showing the residuals, showing the sum of the fit components, the Abbe criterion [10–12], uniqueness plots [13], peak smoothing/denoising, e.g., by wavelets [14,15], chemometrics tools such as principal component analysis, multivariate curve resolution, and pattern recognition entropy [16], and width functions [17,18].

2. Results and discussion

2.1. Basic theory of convolution and the GLS and GLP functions

When peak fitting an XPS narrow scan, one generally selects a baseline first followed by a series of peaks (usually synthetic fit components) that represents the chemical/oxidation states [2] of an element. We noted above that some of the most common functions chosen to represent symmetric XPS signals are the Gaussian, Lorentzian, Gaussian-Lorentzian sum (GLS), Gaussian-Lorentzian product (GLP), and Voigt functions. We now discuss these functions in some detail.

Gaussian and Lorentzian functions play extremely important roles in science, where their general mathematical expressions are given here in Eqs. (1) and (2), respectively [19,20,12].

$$G(x;F,E,h) = h * \exp\left[-4\ln 2\,\frac{(x-E)^2}{F^2}\right] \quad (1)$$

$$L(x;F,E,h) = \frac{h}{\left[1+4\,\frac{(x-E)^2}{F^2}\right]} \quad (2)$$

These Gaussian and Lorentzian functions are graphed in Figs. 1 and 2, respectively, with the following parameters: h = 1 (the functions have a height of one), E = 0 (the functions are centered at the origin), and F = 1 (the functions have a width of one). Note that Eqs. (1) and (2) and many of those below follow the formatting of Fairley [19]. Obviously both functions are symmetric about their center points. They also have finite integrals and are localized – they do not have exceedingly large tails or other components that extend out to a significant degree. The Gaussian curve is the classic 'bell-shaped' or 'normal' curve/distribution. The Lorentzian is somewhat narrower around its maximum and it extends out a little more than the Gaussian on its sides, i.e., the Lorentzian has 'wings'. Any serious physical scientist should know the difference between these two functions, be able to recognize their shapes, and be comfortable working with them.

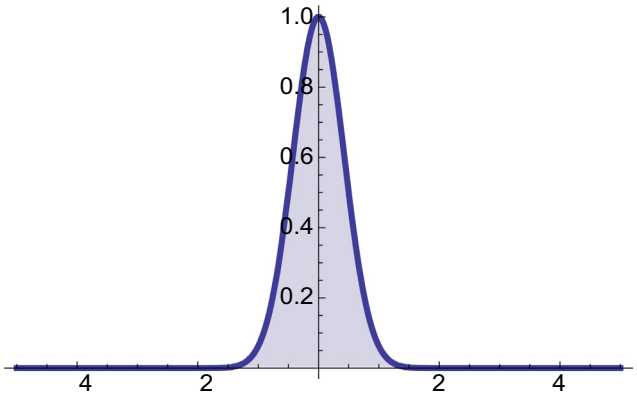

Fig. 1. The Gaussian function from Eq. (1) with parameters h = 1, E = 0, and F = 1.

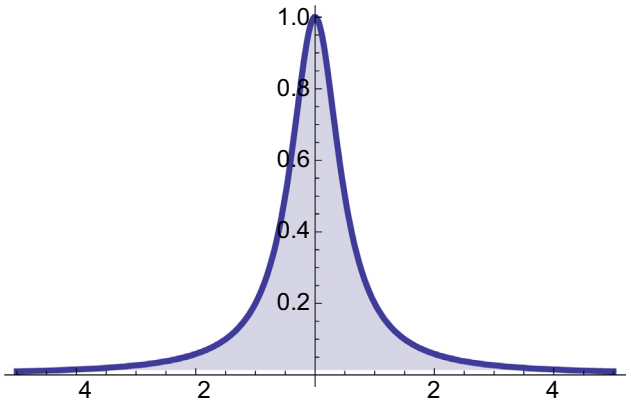

Fig. 2. The Lorentzian from Eq. (2) with parameters h = 1, E = 0, and F = 1.

In the theory of X-ray photoelectron spectroscopy, natural line shapes are generally assumed to be Lorentzian. There are, however, reasons why this line shape may not be observed experimentally. There will be some line width of the X-rays that excite the photoelectrons, i.e., they won't be perfectly monochromatic. The photoelectrons will travel through a spectrometer that will broaden signals to some degree. The elements in question within a sample may be in heterogeneous environments (disorder broadening), and the emission of the photoelectrons may be perturbed by vibrations in the material (phonon broadening), which is temperature dependent. For a more detailed discussion of these concepts, see Briggs and Grant's book on Surface Analysis [19]. One can think of at least some of these broadening mechanisms as being convolutions of the natural, Lorentzian, line shape with other functions, often Gaussians. (MRL previously published a tutorial article on convolution in Vacuum Technology & Coating. This document is included in the Supporting Information of this article [21].) In mathematics, the Central Limit Theorem states that it will often be the case that if a function is repeatedly convolved with itself, or if a series of functions are convolved together, the resulting function will increasingly resemble a Gaussian. This function will also become increasingly smooth and broad. We now illustrate these concepts with the slit function, S(x), shown in Fig. 3. This function is important enough to be referred to in other ways, including as Π(x), Rect (x), or simply as the rectangle function [22]. S(x) is an important window, or apodization, function in signal processing, i.e., it has a value of zero outside of a specific interval. In addition, there are a number of interesting relationships between S(x) and other common functions in signal processing, e.g., it can be derived from the unit step function, θ(x) (Eq. (3)), where S(x) is the product of θ (½ − x) and θ(x + ½) (see Eq. (4)). Note that it rarely matters how functions like θ(x) and S(x) are defined at their transition points. For example, if we redefined θ(x) as 1 for x > 0 and 0 for x ≤ 0, it would only differ from the definition in Eq. (3) by a null function,

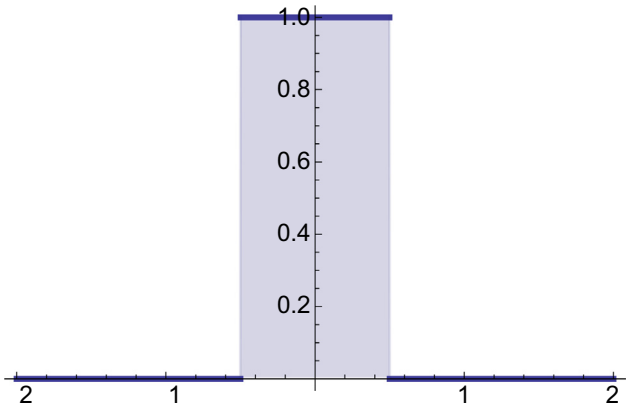

Fig. 3. Graph of the slit function, S(x), with a width of 1.

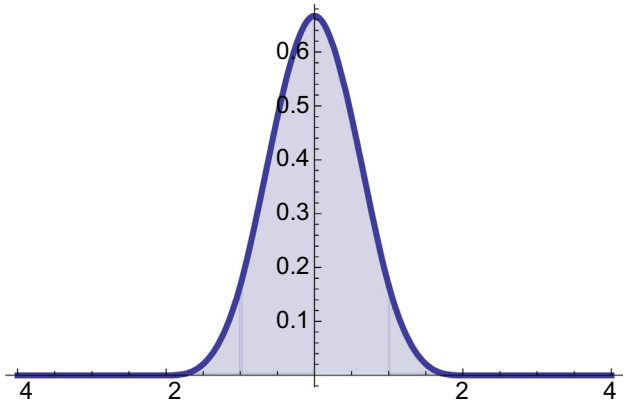

Fig. 5. Convolution of the triangle function with itself (T(x) * T(x)) forming a function that appears rather Gaussian-like.

i.e., for all practical purposes these functions will behave identically.

$$UnitStep(x) = \theta(x) = \begin{cases} 1 & for\ x \geqslant 0 \\ 0 & for\ x < 0 \end{cases} \quad (3)$$

$$S(x) = \theta\left(\frac{1}{2} - x\right)\theta\left(x + \frac{1}{2}\right) = \begin{cases} 1 & for\ x \leqslant \frac{1}{2} \\ 0 & for\ x > \frac{1}{2} \end{cases} \quad (4)$$

Now, if we convolve S(x) with itself (S(x) ∗ S(x)) we get the triangle function, T(x), shown in Fig. 4. (Note that the triangle function may also be represented as Λ(x).) Of course this function is still somewhat angular – it consists of line segments, however it can be argued that it is beginning to resemble a Gaussian function and that it does so to a greater degree than S(x). It also seems to be getting smoother. That is, would you rather drive over bumps on a road shaped like the features in Fig. 3 or Fig. 4? A more advanced justification for stating that S(x) is smoother than T(x) is to note that it only takes one derivative to reduce S(x) to delta (impulse) functions, while it takes two derivatives to reduce T(x) to these types of functions. Finally, note that the convolution of S(x) with itself, T(x), is broader that S(x), i.e., S(x) has non-zero values between −½ and ½, while, T(x) has non-zero values between −1 and 1.

We now convolve T(x) with itself, where T(x) ∗ T(x) = T(x) ∗ S(x) ∗ S(x) = S(x) ∗ S(x) ∗ S(x) ∗ S(x). The resulting function is shown in Fig. 5. Consistent with the Central Limit Theorem it is starting to look rather Gaussian-like – this function is smoother and broader than its predecessor in Fig. 4. Thus, it would be reasonable to expect that it would require more derivatives to reduce T(x) ∗ T(x) to a series of impulse functions than T(x) or S(x). All of this is to argue for the reasonableness of stating that when a set of photoelectrons, which may inherently have a Lorentzian line shape, is perturbed by a spectrometer and/or the broadening mechanisms mentioned above, one would expect the final signal to have at least some Gaussian character. Thus, the recommendation [3] that the C 1s fit components of polymers be modeled as 100% Gaussians or 90:10 Gaussian:Lorentzian mixes seems reasonable because polymers will often exist in rather heterogeneous environments, i.e., their chains can often be approximated as random coils, which will correspond to a variety of bond angles and chemical environments for the different chemical groups/moieties within the polymer. Note that the photoemission spectra from this example in the Literature were collected on an older XPS instrument. In general, newer instruments produce signals with more Lorentzian character, i.e., this suggestion is no longer entirely current. Also, peaks generated from polymeric materials with newer instruments generally show some asymmetry in their shapes.

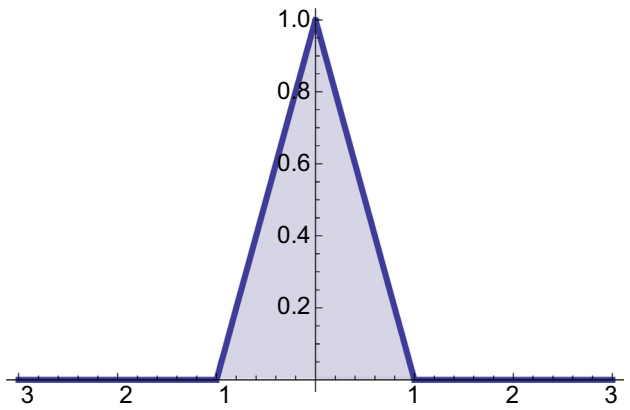

Fig. 4. Convolution of the slit function in Eq. (4), with itself (S(x) * S(x)) forming a triangle function, T(x).

A more advanced and precise mathematical justification for the peak broadening mechanisms discussed herein is to note that variances add under convolution. That is, for two functions f and g with variances σ_f and σ_g, their convolution (f*g) has a variance σ_{f*g} given by:

$$\sigma^2_{f*g} = \sigma^2_f + \sigma^2_g \quad (5)$$

For example, the convolution of a Gaussian with a second Gaussian is yet an additional Gaussian, where according to Eq. (5), this new Gaussian will be broader than either of the original Gaussians.

So we have argued that it is plausible that many of the components of XPS narrow scans will be best defined and fit by peaks that have both Gaussian and Lorentzian character. Mathematically, the 'purest' way to handle this problem is to use a Voigt function, which is the convolution of a Gaussian and a Lorentzian. Historically, however, this convolution was found to be computationally expensive so many of the earlier XPS fitting packages used one of two approximations for it: the Gaussian-Lorentzian sum (GLS) or the Gaussian-Lorentzian product (GLP) function. These functions remain relevant today because (i) there are still a number of fitting packages that provide the GLS and/or the GLP functions as options, (ii) there is a great deal of Literature precedent for the use of both of these functions, and (iii) these functions work – both the Literature and the examples provided below show that both the GLS and the GLP remain useful and relevant in peak fitting. Indeed, it is an active area of research to determine which synthetic function is most appropriate in different situations.

The GLS function has the following form:

$$GLS(x;F,E,m,h) = h*(1-m)\exp\left[-4\ln 2\frac{(x-E)^2}{F^2}\right] + \frac{h*m}{\left[1+4\frac{(x-E)^2}{F^2}\right]} \quad (6)$$

Notice that the first and second terms in this function are the Gaussian and Lorentzian functions in Eqs. (1) and (2) weighted by a mixing parameter, m. That is, for $m = 0$, Eq. (6) reduces to Eq. (1), a Gaussian, and for $m = 1$, Eq. (6) reduces to Eq. (2), a Lorentzian. Obviously, by varying m from 0 to 1 we can proceed from a pure Gaussian to a pure Lorentzian function. Clearly, m could be a parameter in an algorithm used to fit XPS narrow scans. Fig. 6 shows the GLS function (Eq. (6)) for three values of m: $m = 0$ (the blue/bottom line), which (again) is a Gaussian, $m = 1$ (the yellow/top line), which is a Lorentzian, and $m = 0.5$ (the red/middle line), which runs between the other two functions. Fig. 7 goes a little further, zooming in on the region where the Gaussian and Lorentzian functions differ and showing results for $m = 0$, 0.1, 0.3, 0.5, 0.7, and 1. It is clear that the GLS allows variation in a reasonable way between a pure Gaussian and a pure Lorentzian function.

The GLP function is defined in Eq. (7). As expected from its name, it consists of the product of a Gaussian and a Lorentzian function. As was the case for the GLS, the GLP contains a mixing parameter, m, and values of $m = 0$ and $m = 1$ in Eq. (7) yield pure Gaussian (Eq. (1)) and pure Lorentzian functions (Eq. (2)), respectively.

$$GLP(x;F,E,m,h) = h*\exp\left[-4\ln 2(1-m)\frac{(x-E)^2}{F^2}\right] * \frac{1}{\left[1+4m\frac{(x-E)^2}{F^2}\right]} \quad (7)$$

At this point, it may appear that the GLS and GLP functions are interchangeable, but this is not the case. Fig. 8 shows the GLP function for $m = 0$, 0.5, and 1. It is clear here that while the $m = 0.5$ GLS function was approximately in the middle of the pure Gaussian and Lorentzian functions (see Fig. 6), the $m = 0.5$ GLP function differs only slightly from the pure Gaussian. The obvious reason for this is that, as suggested above, the Gaussian function is 'more contained' than the Lorentzian function – it goes to zero faster. As a result, when the Lorentzian and Gaussian functions in Fig. 8 are multiplied together, the 'wings' of the Lorentzian are multiplied by values that are quite close to zero with the result that they largely disappear. These conclusions are further confirmed in Fig. 9, which shows an enlarged view of the $m = 0.5$ GLP function and also

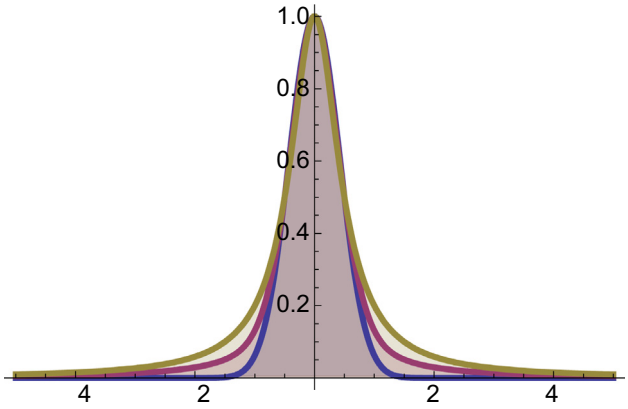

Fig. 6. Graph of the GLS function (Eq. (5)) with parameters h = 1, E = 0, and F = 1 for m = 0 (bottom, blue line), m = 0.5 (middle, red line), and m = 1 (top, yellow line). (For interpretation of the references to colour in this figure legend, the reader is referred to the web version of this article.)

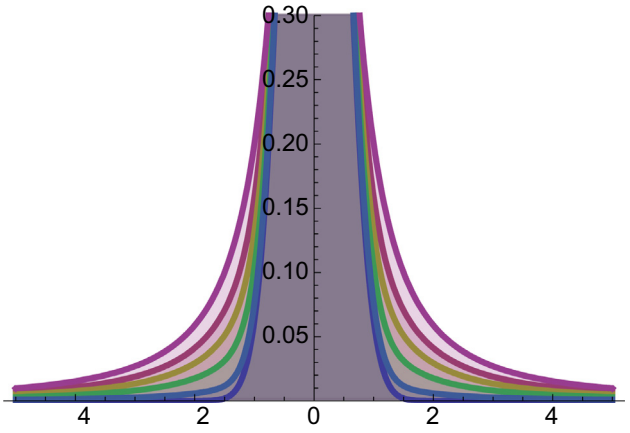

Fig. 7. Graph of the GLS function (Eq. (3)) with parameters h = 1, E = 0, and F = 1 for (from bottom to top) m = 0, 0.1, 0.3, 0.5, 0.7, and 1.

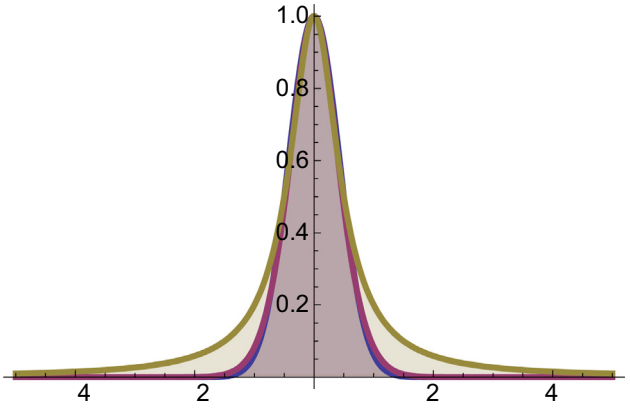

Fig. 8. Graph of the GLP function (Eq. (7)) with parameters h = 1, E = 0, and F = 1 for m = 0 (bottom, blue line), m = 0.5 (middle, red line), and m = 1 (top, yellow line). (For interpretation of the references to colour in this figure legend, the reader is referred to the web version of this article.)

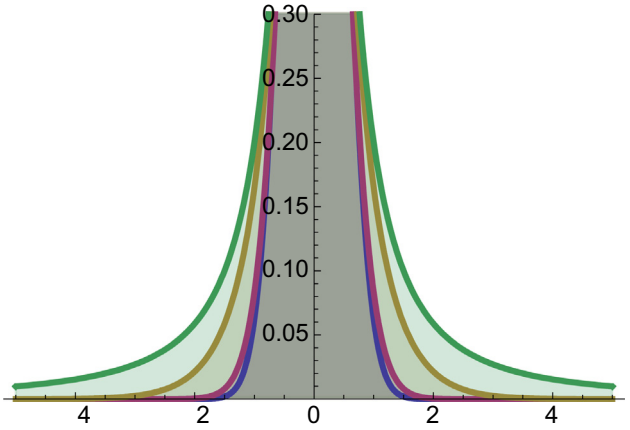

Fig. 9. Graph of the GLP function (Eq. (7)) with parameters h = 1, E = 0, and F = 1 for, going from bottom to top, m = 0 (blue line), m = 0.5 (red line), m = 0.9 (yellow line), and m = 1 (green line). (For interpretation of the references to colour in this figure legend, the reader is referred to the web version of this article.)

of the m = 0.9 GLP function. A priori, one might expect that a mixing parameter of 0.9 would yield a GLP function that would rather closely resemble/follow a pure Lorentzian function. However, even at m = 0.9 the GLP function only appears to be about half way between the pure Gaussian and pure Lorentzian, where this representation/extension of the function still poorly represents the 'wings' of the Lorentzian, cf., Fig. 7.

For comparison to the use of m in this work, four XPS instrument manufacturers and an XPS software company were surveyed to determined how they handle the mixing parameter in the Gaussian-Lorentzian mixture functions in their software. Four of the companies: CasaXPS (UK), Kratos (Manchester, England), Specs (Berlin, Germany), and ThermoFisher (East Grinstead, UK) use m = 0 for the pure Gaussian and m = 1 for the pure Lorentzian. Interestingly, the default peak for peak fitting in the software package of one of these XPS companies is a GLP with m = 0.3. Fig. 8 suggests that this synthetic peak shape is very nearly a Gaussian. Also, m is presented in two of these software packages as a percentage running from 0 to 100 (see, for example, the peak fits in the Supporting Information that were performed in CasaXPS). However, PHI (Chanhassen, MN) takes the opposite approach, using m = 0 for its pure Lorentzian. Beamson and Briggs similarly used a GLS with m = 0 corresponding to a pure Lorentzian and m = 1 to a pure Gaussian [23].

Around 1980, the GLP function was recommended in the literature for XPS narrow scan peak fitting [24]. This suggestion appears to have been relatively influential. However, a later paper in 2007 by Hesse, Streubel, and Szargan [12] did not confirm the previous recommendation. In their analyses of synthetic, Voigt-based XPS spectra, i.e., they did not use real data, the GLS function mathematically/theoretically outperformed the GLP. In their work, Hesse and coworkers plotted the GLS with m = 0.5, the GLP with m = 0.5, and the Voigt function, all with widths of 2. This plot is reproduced in Fig. 10, albeit with the peaks shifted to the origin so they can be better compared to the peaks in the other figures in this document. The Voigt function (yellow line) is the widest of the three functions. The red line just inside it is the GLS function. Obviously the GLS function approximates the Voigt function quite well. The lowest line in Fig. 10 is the GLP. It is clearly a less adequate approximation of the Voigt function. In 2003, Fairley also discussed this issue, noting, as had Hesse, the significant decrease of the Lorentzian's wings when it is multiplied by a Gaussian [19,10].

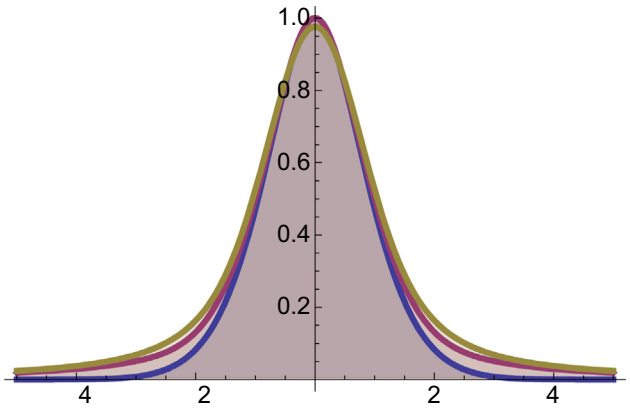

Fig. 10. Graphs of the GLS function with m = 0.5 (red line), the GLP function with m = 0.5 (blue line), and the Voigt function (yellow line). All three functions have widths of 2 and are centered at the origin. The Voigt function here is the convolution of a Gaussian function with a width of 1.3 and a Lorentzian function with the same width. A figure similar to this one previously appeared in paper by Hesse and coworkers [12]. (For interpretation of the references to colour in this figure legend, the reader is referred to the web version of this article.)

2.2. Practical applications of the GLP and its comparison to the GLS function

At this point one might argue that the GLS should be favored and the GLP deprecated, where the mathematical reasoning outlined and cited here is supportive of this position. However, at some point, the most important test of a synthetic line shape is not the theory behind it but rather its effectiveness in fitting real data. As shown in this section, the GLP appears to more effectively fit some XPS narrow scans, which indicates that it remains a useful synthetic line shape for XPS narrow scan analysis. Modern XPS instruments have seen an increase in energy resolution for both the spectrometer and X-ray source. As the spectral resolution contributions from the spectrometer and source, which are both Gaussian in shape, decrease, an increase in the resolution contribution from the core-line, which is Laurentian in shape, is seen (barring other effects as mentioned earlier).

The three examples below illustrate the use of the GLP in XPS narrow scan analysis. The spectra and fits corresponding to these analyses, which were performed in CasaXPS, are in the Supporting Information. Note that 'GL' and 'SGL' in CasaXPS are the same as GLP and GLS, respectively, in this work.

(a) The first example shows an Mo 3d spectrum from a sample of MoO_3. The two signals here are the Mo $3d_{5/2}$ and $3d_{3/2}$ peaks. They are expected to be mostly Gaussian in nature and are due to spin-orbit splitting. These same peaks with the same Shirley background and similar background endpoints were best fit with a GLP with m = 29 and a GLS with m = 5. The fit residual values for these fits were very similar: 2.539 and 2.699, respectively. The fitting functions here do not differ much from pure Gaussians, and for all practical purposes the fits are identical.
(b) The second example shows the S 2p spectrum from MoS_2. These spin-orbit signals (the S $2p_{3/2}$ and $2p_{1/2}$) are expected to have more Lorentzian character than the signals in the previous example. Best fits to these peaks were obtained with a GLP with m = 62 and a fit residual value of 1.758 and a GLS with m = 17 and a fit residual value of 2.079. Here the GLS is not able to fit the data as well as the GLP.
(c) The third example is the Cu $2p_{3/2}$ signal from a sample of sputter-cleaned metallic copper. Best fits to this peak were obtained with a GLP with m = 60 and a fit residual of 3.931 and a GLS with m = 80 and a fit residual of 1.804. The GLS does a very poor job here and is unable to fit this experimental line shape. Quantitation with the GLS here would be problematic.

Thus we see the practical value of having multiple synthetic line shapes at our disposal for XPS narrow scan analysis.

3. Conclusions

In this article we have discussed a series of line shapes that are important for XPS peak fitting. These include the Gaussian, Lorentzian, GLS, GLP, and Voigt functions, which are discussed and/or presented symbolically in the context of signal processing mathematics, e.g., convolution. Plots of the GLS and GLP are shown with different values of the mixing parameter, m. The parameter m is defined differently by different XPS hardware and/or software companies. Plots of the GLS show that it is a better mathematical representation of a function that is intermediate between a pure Gaussian and a pure Lorentzian. The GLS also appears to be a better approximation of the Voigt function. Because of the more compact nature of the Gaussian, the GLP does not have significant 'wings',

and for low values of m it is a rather close approximation of a pure Gaussian. Nevertheless, as illustrated with three examples, the GLP is also a useful synthetic line shape for XPS narrow scan peak fitting.

Acknowledgments

In February, 2014 one of the authors of this work (MRL) wrote an article in a trade/technical magazine, Vacuum Technology & Coating (VT&C), on 'The Gaussian-Lorentzian Sum, Product, and Convolution (Voigt) Functions Used in Peak Fitting XPS Narrow Scans, and an Introduction to the Impulse Function" [25]. After publishing this article, MRL posted a copy of it to his Research Gate page, where, according to Wikipedia, Research Gate is: "a social networking site for scientists and researchers to share papers, ask and answer questions, and find collaborators." He had not anticipated that this article would receive any special attention. However, as of March 15, 2018 it had received 4137 reads – far more than most of his other articles. This unexpected and enthusiastic response prompted this submission. Accordingly, with the permission of Vacuum Technology & Coating, we present this article, which has been reformatted for this journal, reedited, and more thoroughly referenced. VT&C also approved the use of another of MRL's articles in the Supporting Information. Varun Jain, one of MRL's graduate students, took on the task of adapting the original article. His contributions have been significant. Note that the position taken by MRL in the VT&C article was that the GLP should be avoided for mathematical reasons. This article represents his/our latest thinking on this topic.

Appendix A. Supplementary material

Supplementary data associated with this article can be found, in the online version, at https://doi.org/10.1016/j.apsusc.2018.03.190.

References

[1] J.F. Watts, J. Wolstenholme, An Introduction to Surface Analysis by XPS and AES, John Wiley & Sons Ltd, Chichester, UK, 2005.
[2] V. Gupta, H. Ganegoda, M.H. Engelhard, J. Terry, M.R. Linford, Assigning oxidation states to organic compounds via predictions from X-ray photoelectron spectroscopy: a discussion of approaches and recommended improvements, J. Chem. Educ. 91 (2) (2014) 232–238.
[3] B.V. Crist, Advanced peak-fitting of monochromatic XPS spectra, J. Surface Anal. 4 (3) (1998) 428–433.
[4] P.M.A. Sherwood, Curve fitting in surface analysis and the effect of background inclusion in the fitting process, J. Vacuum Sci. Technol. A: Vacuum, Surfaces, Films 14 (3) (1996) 1424–1432.
[5] G. Beamson, D. Briggs, High-resolution monochromated X-ray photoelectron-spectroscopy of organic polymers – a comparison between solid-state data for organic polymers and gas-phase data for small molecules, Mol. Phys. 76 (4) (1992) 919–936.
[6] S. Doniach, M. Sunjic, Many-electron singularity in X-ray photoemission and X-ray line spectra from metals, J. Phys. C: Solid State Phys. 3 (2) (1970) 285.
[7] H. Ganegoda, D.S. Jensen, D. Olive, L.D. Cheng, C.U. Segre, M.R. Linford, J. Terry, Photoemission studies of fluorine functionalized porous graphitic carbon, J. Appl. Phys. 111 (5) (2012) 053705.
[8] B. Singh, R. Hesse, M.R. Linford, Good Practices for XPS (and other Types of) Peak Fitting, Use Chi Squared, Use the Abbe Criterion, Show the Sum of Fit Components, Show the (Normalized) Residuals, Choose an Appropriate Background, Estimate Fit Parameter Uncertainties, Limit the Number of Fit Parameters, Use Information from Other Techniques, and Use Common Sense. Vacuum Technology & Coating, December, 2015.
[9] B. Singh, A.H. Gomez, J. Terry, M.R. Linford, Good Practices for XPS Peak Fitting, II Vacuum Technology & Coating, August 2016.
[10] R. Hesse, T. Chasse, P. Streubel, R. Szargan, Error estimation in peak-shape analysis of XPS core-level spectra using UNIFIT 2003: how significant are the results of peak fits?, Surface Interface Anal 36 (10) (2004) 1373–1383.
[11] R. Hesse, T. Chasse, R. Szargan, Peak shape analysis of core level photoelectron spectra using UNIFIT for WINDOWS, Fresenius J. Anal. Chem. 365 (1–3) (1999) 48–54.
[12] R. Hesse, P. Streubel, R. Szargan, Product or sum: comparative tests of Voigt, and product or sum of Gaussian and Lorentzian functions in the fitting of synthetic Voigt-based X-ray photoelectron spectra, Surface Interface Anal. 39 (5) (2007) 381–391.
[13] B. Singh, A. Diwan, V. Jain, A. Herrera-Gomez, J. Terry, M.R. Linford, Uniqueness plots: a simple graphical tool for identifying poor peak fits in X-ray photoelectron spectroscopy, Appl. Surface Sci. 387 (2016) 155–162.
[14] C. Charles, G. Leclerc, J.-J. Pireaux, J.-P. Rasson, Introduction to wavelet applications in surface spectroscopies, Surface Interface Anal. 36 (1) (2004) 49–60.
[15] C. Charles, G. Leclerc, P. Louette, J.-P. Rasson, J.-J. Pireaux, Noise filtering and deconvolution of XPS data by wavelets and Fourier transform, Surface Interface Anal. 36 (1) (2004) 71–80.
[16] S. Chatterjee, B. Singh, A. Diwan, Z.R. Lee, M.H. Engelhard, J. Terry, H.D. Tolley, N.B. Gallagher, M.R. Linford, A perspective on two chemometrics tools: PCA and MCR, and introduction of a new one: Pattern recognition entropy (PRE), as applied to XPS and ToF-SIMS depth profiles of organic and inorganic materials, Appl. Surface Sci. 433 (2018) 994–1017.
[17] B. Singh, D. Velazquez, J. Terry, M.R. Linford, Comparison of the equivalent width, the autocorrelation width, and the variance as figures of merit for XPS narrow scans, J. Electron Spectrosc. Related Phenomena 197 (2014) 112–117.
[18] B. Singh, D. Velazquez, J. Terry, M.R. Linford, The equivalent width as a figure of merit for XPS narrow scans, J. Electron Spectrosc. Related Phenomena 197 (2014) 56–63.
[19] N. Fairley, in: Surface Analysis by Auger and X-Ray Photoelectron Spectroscopy, IM Publications, UK, 2003, pp. 397–403.
[20] N. Fairley, Peak Fitting in XPS, www.casaxps.com. UK, 2006.
[21] M.R. Linford, An introduction to convolution with a few comments beforehand on XPS, Vacuum Technology & Coating (June 2014), 25–31.
[22] R.N. Bracewell, Fourier Transform and Its Applications, 3rd ed., McGraw-Hill Companies, USA, 1999.
[23] G. Beamson, D. Briggs, High Resolution XPS of Organic Polymers-The Scienta ESCA300 Database, Wiley Interscience, USA, 1992, p. 31.
[24] P.M.A. Sherwood, Practical Surface Analysis, John Wiley Chichester, England, 1983.
[25] M.R. Linford, The Gaussian-Lorentzian Sum, Product, and Convolution (Voigt) Functions Used in Peak Fitting XPS Narrow Scans, and an Introduction to the Impulse Function, Vacuum Technology & Coating, July, 2014, pp. 27–33.